The Journal of the Oceanological Society of Korea
Vol. 28, No. 3, pp. 177-185, September 1993

Scattering of a Kelvin Wave by a Cylindrical Island

SANG HO LEE* AND KUH KIM**
*Department of Oceanography, Kunsan National University, Kunsan, 573-360
**Department of Oceanography, Seoul National University, Seoul, 151-742

원통형 섬에 의한 Kelvin 파의 산란

이상호* · 김 구**
*군산대학교 해양학과
**서울대학교 해양학과

The theory for long wave scattering (Proudman, 1914; Longuet-Higgins, 1970) is applied to a tidal-frequency Kelvin wave propagating around a small cylindrical island in a shelf sea of uniform depth. The theory includes the effects of bottom friction on wave propagation. The theoretical analysis shows that the amplitude of the scattered wave contributes to change the rate of amplitude decay of the Kelvin wave around the island. This amplitude change results in a uniform amplitude of the total wave along the circumference of the island in an inviscid fluid, and the dynamic cause of this is explained in terms of Coriolis effects. Bottom friction attenuates the amplitude of the total wave from the frontal side of the island to the leeward side, but the amplitude variation along the coast becomes symmetric to the line connecting both sides. The phase of the scattered wave contributes to more rapid travel of the total wave in the front and leeward side than farther offshore. The effects of bottom friction on the wave phase around the island are negligible.

장파의 산란이론(Proudman, 1914; Longuet-Higgins, 1970)을 대륙붕상의 작은 원통형 섬주변을 전파하는 조석주기의 Kelvin파에 적용하였으며, 해저마찰의 효과를 포함하였다. 이론적 분석에 의하면 산란파의 진폭은 섬주변에서 Kelvin 파의 진폭 감소율을 변화시킨다. 이러한 진폭의 변화로 비점성 유체의 경우에 섬 연안을 따라 진폭이 균등해지고, 진폭변화는 전향력의 작용으로 설명되어진다. 해저마찰력은 파가 전파되어 오는 쪽 연안에서 전파되어가는 쪽 연안으로 진폭을 감쇄시키나, 연안을 따른 진폭변화는 상기 연안을 연결하는 선에 대하여 대칭이다. 산란파의 위상은 외해에 비해 전파되어오고 가는 쪽 연안 부근에서 파의 진행이 빨라지게 한다. 섬 주변에서 파의 위상분포에 미치는 해저면 마찰력의 영향은 무시할만 하다.

INTRODUCTION

Propagation of tidal waves around an island produces an appreciable local modification of the amplitude and phase. For example, Larsen (1977) showed that scattering alters the time of high water around Hawaii by as much as an hour. Kim and Lee (1986) and Lee and Kim (1988) found that amplitudes of the semidiurnal (M_2, S_2) and diurnal ztides (O_1, K_1) vary with geographical locations around the circumference of Cheju Island. They showed that for an observer facing the direction of tidal propagation, the tidal amplitudes on the left-hand coast are larger than those on the right-hand coast around Cheju Island. This amplitude variation across the island is opposite to the general trend of the tidal amplitudes decreasing southward off the southern coast of Korea.

For tides around Hawaii Islands with periods shorter than the local inertial period Larsen(1977) applied an approximate solution for scattering of Sverdrup(plane) wave by Proudman(1914). Adopting a similar theoretical model Kim and Lee(1986) interpreted the amplitude variation of semidiurnal tides around Cheju Island. However, periods of diurnal tides are longer than the local inertial period around Cheju Island, which is 21.7 hours. Therefore, the observed variation of O_1 and K_1 tides around Cheju Island remains to be explained, as the propagation of the Sverdrup wave in an inviscid fluid is not supported for subinertial frequencies.

In shelf seas, Kelvin wave is a major propagator of tidal energy (Platzman, 1971), and subinertial-frequency tides can propagate as Kelvin waves (Pedlosky, 1979). The objective of this paper is to apply Proudman's (1914) theory to Kelvin wave scattering around a circular cylindrical island, in which wave-like solutions are allowed without any limitations on frequency, and to examine the variation of amplitude and phase by the scattering around the island.

Proudman (1914) derived analytical solutions for the long wave scattering by an island and a cape in an inviscid fluid, and showed that the approximate solution is valid near the obstacle. Proudman (1914), however, did not apply his solution to the the case of Kelvin wave scattering by an island. Later, Longuet-Higgins (1970) obtained another approximate solution for the disturbance of an inertial wave by a small island by replacing the Helmholtz wave equation by Laplace's equation, based upon the assumption that the scale of local disturbance by a small island is exceedingly small compared to the external Rossby deformation radius. Larsen (1977) showed that Longuet-Higgins' (1970) method produces the same result as Proudman's (1914) approximation but the former is more direct and convenient.

Bottom friction plays an important role in dissipating the tidal energy in shallow shelf seas. Recently, bottom frictional effects on Kelvin wave propagation were studied by Mofjeld (1980), who pointed out two important effects. First, the wavelengths of Kelvin waves are shortened by friction, and the cophase lines slant backward to the direction of propagation since the offshore wavenumber is nonzero with friction. Second, the alongshore attenuation of amplitude increases with increasing friction, and the offshore decay scale can be smaller than the Rossby radius.

In this paper, the long-wave equation is linearized with the Rayleigh form of bottom friction and the method by Longuet-Higgins (1970) is used to derive the scattering solution for the Kelvin wave propagating around a cylindrical island. The dynamical explanation and examples of the amplitude and phase field for the wave modification with scattering will be described in detail.

THEORY

Wave equation

The linearized equations (Le Blond and Mysak, 1978) for long waves with a linear bottom friction in a sheet of water of uniform depth h take the form

$$\underline{u}_t + \underline{f}\times\underline{u} = -g\nabla\zeta - C_b\underline{u}/h, \qquad (1)$$
$$\zeta_t + h\nabla\cdot\underline{u} = 0,$$

where $\underline{u}$ is the vertically-averaged horizontal velocity vector, ζ is the surface elevation, $\underline{f}$ is the Coriolis parameter constant in vertical direction, ∇ is the horizontal gradient and C_b is the linear coefficient representing the effect of bottom friction. Assuming a time factor $\{\zeta, \underline{u}\} = \mathrm{Re}\{(Z, \underline{U})\exp(-i\omega t)\}$ at a given wave frequency $\omega>0$, the wave equations may be deduced to the following Helmholtz equation

$$\nabla^2 Z + k^2 Z = 0, \qquad (2)$$

$$\underline{U} = -g/(\sigma^2+f^2)\ (\sigma\nabla Z - \underline{f}\times\nabla Z), \qquad (3)$$

where

$$\sigma = \omega(1 - i\tau), \qquad (4)$$

$$k^2 = i\omega(\sigma^2 + f^2)/\sigma gh, \qquad (5)$$

$$\tau = C_b/h. \qquad (6)$$

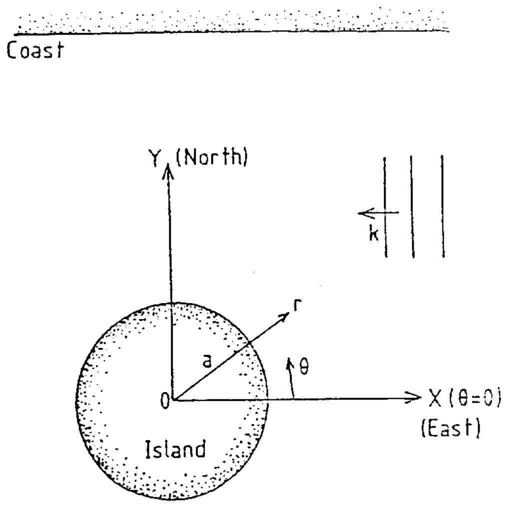

Fig. 1. Coordinates system on the cylindrical circular island with radius a and the propagating direction of incident Kelvin wave.

For barotropic Kelvin waves to exist, it is assumed that a straight east-west coast is located north of the island(Fig. 1), and the offshore velocity is taken as zero (i.e., $v=0$). In this case, the direction of primary (incident) wave propagation is the negative x-direction, and the dispersion relation (5) yields the complex wavenumbers

$$k_x = -(i\omega\sigma/gh)^{1/2},\quad k_y = fk_x/\sigma. \tag{7}$$

The component parts of these complex wave-numbers are defined as follows: $\alpha=\mathrm{Re}(k_x)$ is the alongshore wavenumber, $\beta=\mathrm{Im}(k_x)$ is the alongshore-damping coefficient of wave amplitude, $m=\mathrm{Re}(k_y)$ is the offshore wavenumber, and $n=\mathrm{Im}(k_y)$ is the offshore-decay coefficient of wave amplitude. These four components have negative values in our case. This paper attempts to find a solution for the scattering of this incident Kelvin wave around a cylindrical island of radius (a), where $\alpha_o \ll 1$.

Wave scattering

The Helmholtz equation (2) takes the form in the polar coordinates $(r^2\partial^2/\partial r^2 + r\partial/\partial r + \partial^2/\partial\theta^2 + k^2 r^2)$ $Z=0$, where r is the distance from the island center and is the angle measured counterclockwise from the east. Near the small island, $|kr|$ so that (2) can be reduced to Laplace's equation

$$\nabla^2 Z = 0. \tag{8}$$

In this case, the primary Kelvin wave (Z_o) can be represented near the island by

$$\begin{aligned} Z_o &= \exp(ik_x x + ik_y y) \\ &\simeq 1 + ik_x r(\cos\theta + f/\sigma\sin\theta) \\ &= 1 - r(n\sin\theta + \beta\cos\theta) + ir(m\sin\theta + \alpha\cos\theta). \end{aligned} \tag{9}$$

This island will scatter the primary Kelvin wave. If the wave energy radiating from the island is assumed to be constant within the circle of radius r from the island, the amplitudes of the scattered wave will be reversely proportional to the distance r. With this assumption, the scattered wave (Z_s) near the island can take the form

$$Z_s = 1/r\ (B\ \sin\theta + C\ \cos\theta). \tag{10}$$

The superposition of primary and scattered waves composes the total wave $Z=Z_o+Z_s$ which must satisfy (8) around the island.

The boundary condition of no normal flow at the coast of the island can be written in polar coordinates

$$\begin{aligned} U_r &= U\cdot r \\ &= (\sigma\nabla Z - f\times\nabla Z)\cdot r \\ &= (\sigma\partial/\partial r + f\partial/r\partial\theta)\ (Z_o + Z_s) \\ &= 0,\ \text{at}\ r=a. \end{aligned} \tag{11}$$

It is assumed that the straight coast is located so far from the island that the amplitude of the scattered wave is negligible at that coast. This implies that the reflected wave from the straight coast does not affect the wave field around the island. Thus, (11) is sufficient to solve the Kelvin wave scattering around the island.

Constants B and C in (10) are determined through (11), since $Z=Z_o+Z_s$ must satisfy the boundary condition for any azimuthal direction. After some manipulation, they are obtained as $C=ia^2k_x$ and $B=-ia^2k_y$. The total wave solution with these constants takes the following form

$$\begin{aligned} Z &= 1 + i\{r(k_x\cos\theta + k_y\sin\theta) + a^2/r(k_x\cos\theta - k_y\sin\theta)\} \\ &= 1 - n(r - a^2/r)\sin\theta - \beta(r + a^2/r)\cos\theta \\ &\quad + i\{m(r - a^2/r)\sin\theta + \alpha(r + a^2/r)\cos\theta\} \end{aligned} \tag{12}$$

Since the imaginary part in (12) is much smaller than the real part near the island, the scattering solution to our order of approximation can be represented by

$$\zeta=\{1-n(r-a^2/r)\sin\theta-\beta(r+a^2/r)\cos\theta\}\cos(\omega t+\phi k), \quad (13)$$

$$\phi_k=\alpha(r+a^2/r)\cos\theta+m(r-a^2/r)\sin\theta. \quad (14)$$

Because the amplitude of the primary Kelvin wave is not isotropic, the exponential decay of the amplitude of the primary wave can be reconstructed to its original form: $1-nr\sin\theta-\beta r\cos\theta=\exp(-nr\sin\theta-\beta r\cos\theta)$. The solution (13) for wave scattering is then written as

$$\zeta=\{\exp(-nr\sin\theta-\beta r\cos\theta) + a^2/r(n\sin\theta-\beta\cos\theta)\}\cos(\omega t+\phi_k). \quad (15)$$

Bottom friction produces additional terms including β and m in (13) and (14). If bottom friction is neglected($\beta=0$), the third term in (13) disappears. In this case, the wave amplitude along the circumference of the island ($r=a$) becomes uniform. This result is quite different from the Sverdrup-wave scattering case discussed by Kim and Lee (1986). It should be noticed that the scattering of a Kelvin wave in an inviscid fluid is apparently independent of the island dimension and of the wave frequency as far as our order of approximation is allowed. Meanwhile, bottom friction will cause the amplitude to vary along the coast of the island as a function of cosθ in (13), implying the amplitude attenuation along the direction of wave propagation. The phase of the wave at the coast of the island does not change with wavenumber m, so that the phase varies along the coast as a function of cosθ in (14), whether bottom friction is included or not.

Dynamical considerations

The fluid particle motion in a Kelvin wave is rectilinear, parallel to the direction of wave propagation when bottom friction is zero. The radial and azimuthal currents U_r and U_θ are

$$U_r=-A(1-a^2/r^2)\cos\theta$$

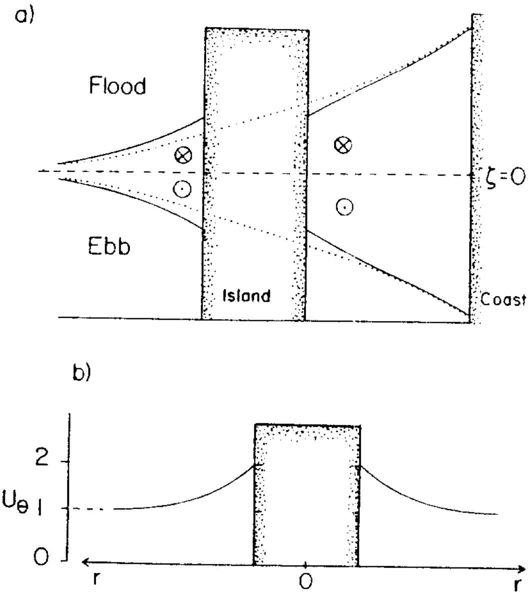

Fig. 2. (a) Schematic cross section of the sea level of Kelvin wave at high and low waters. Dotted lines are the sea level of incident wave. Conventional notations are used for the direction of a current. (b) Schematic cross section of the current amplitude near the island.

$$U_\theta=A(1+a^2/r^2)\sin\theta \quad (16)$$

where $A=igk_y/\sigma$. This current field will be valid near the island. At the coast of the island, the radial current is reduced to zero and azimuthal current is increased as much as twice the farfield magnitude. This current modification near the island occurs concurrently with the modification of the amplitude and phase of the incident Kelvin wave.

To illustrate the dynamical process for amplitude modification near the island, schematic figures are constructed in Fig. 2 for the sea level and current magnitude at high and low water at the north-south section ($\theta=\pi, 3\pi/2$). During flood, the current flows in the direction of wave propagation (into the paper in Fig. 2(a)), and U_θ increases near the island. The Coriolis force on U_θ should balance the radial pressure gradient due to sea surface slope, while the local acceleration of U_θ balances with the azimuthal pressure gradient and bottom friction. In this period the sea level of the primary

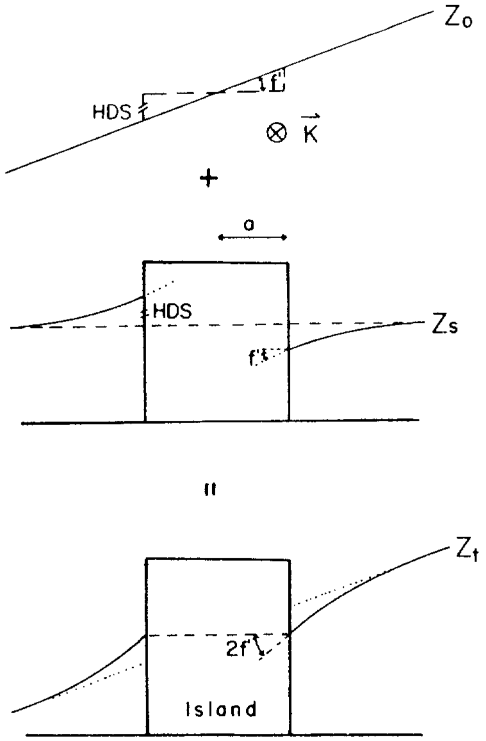

Fig. 3. Component amplitude profiles in a Kelvin wave scattering, top: incident wave, middle: scattered wave, bottom: total wave. Conventional notation is used for the incident wave vector. HDS $=a\times f'$ denotes half of the amplitude difference of incident wave over the distance of the island diameter and $f'=f(gh)^{-1/2}$ is the amplitude slope of incident wave.

wave (dashed line in Fig. 2(a)) falls (rises) on the north (south) coast of the island due to the increased Coriolis acceleration, resulting in the change of real sea level as shown in Fig. 2(a) with solid line. During ebb, the current reverses its direction. The real sea level appears to fall more (less) on the south (north) coast of the island than the primary wave. The net effect of this temporal change of sea level is to reduce the amplitude difference between both coasts of the island.

The above dynamical explanation for Kelvin wave scattering is basically the same as that for Sverdrup wave scattering given by Kim and Lee (1986). However, the scattering of a Kelvin wave without friction produces an uniform amplitude along the circumference of the island. This uniform amplitude needs more explanation. The component amplitude profiles for the same cross section in Fig. 2 are presented in Fig. 3. In our approximation of (9), the amplitude of the primary wave (Z_o) has the slope $|f'|f(gh)^{-1/2}$ in an inviscid fluid, which is the coefficient of amplitude decay n. With this approximation, the amplitude difference across the island becomes $2a|f'|$ (Fig. 3, top). The amplitude of scattered wave in this section is $Z_s=f'a^2/r\ \sin\theta$, obtained from (13). It is positive on the south ($\theta=3\pi/2$) and negative on the north ($\theta=\pi/2$) coast of the island, due to the negative value of f' in our case. The absolute value of Z_s (Fig. 3, middle) becomes f' a at both coasts of the island ($r=a$), where the amplitude slope of Z_s without friction is the same as that of Z_o. The superposition of incident and scattered wave amplitude produces the same amplitude of the total wave at both sides of the island (Fig. 3, bottom).

Examples of Wave Scattering

The preceding theoretical results are applied for a cylindrical circular island with radius $a=25$ km, water depth $h=75$ m, and $f=8.012\times10^{-5}\ \mathrm{sec}^{-1}$ (33° 20′ N). The M_2 tide has an inviscid wavelength longer than 1200 km and an e-folding scale of about 340 km. The wave field is presented in the area 150 km from the center of the island. The coefficient of bottom friction is $C_b=0.106$ cm/sec ($\tau=C_b/h=1.4147\times10^{-5}\ \mathrm{sec}^{-1}$), which produces the same frictional force as the quadratic form with a velocity of 50 cm/sec and a drag coefficient of 0.0025. Calculations for the O1 tidal wave have also been made.

Distributions of M_2 wave field

The incident Kelvin wave is taken to travel from east to west, passing a small island, as shown in Fig.1. The amplitude of the M_2 tide with and without friction is calculated by multiplying (15) by 100 cm. Distributions of total amplitude and phase without bottom friction are presented in Fig 4. The coamplitude and cophase lines farther outside are nearly parallel to each other as in the propa-

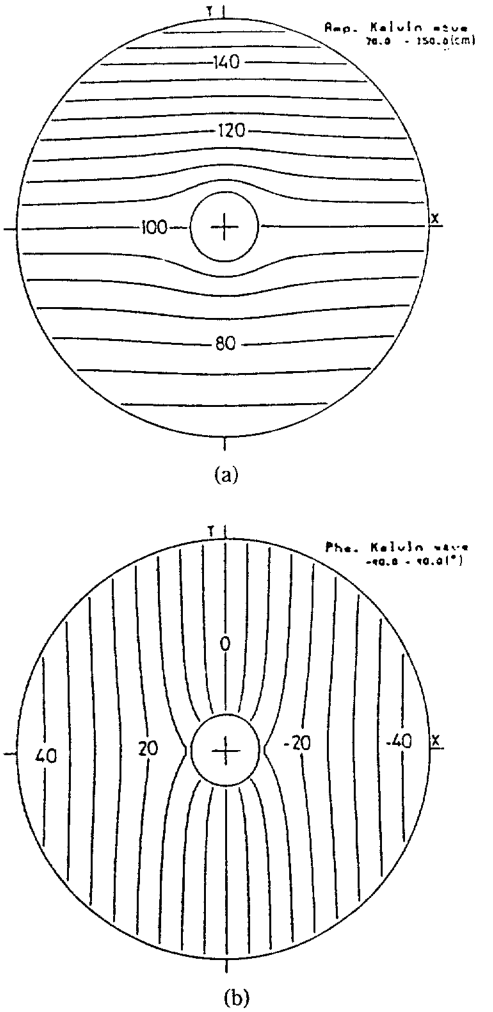

Fig. 4. Distributions of total amplitude (a) and phase (b) by the scattering of the M_2 tidal frequency Kelvin wave in an inviscid fluid.

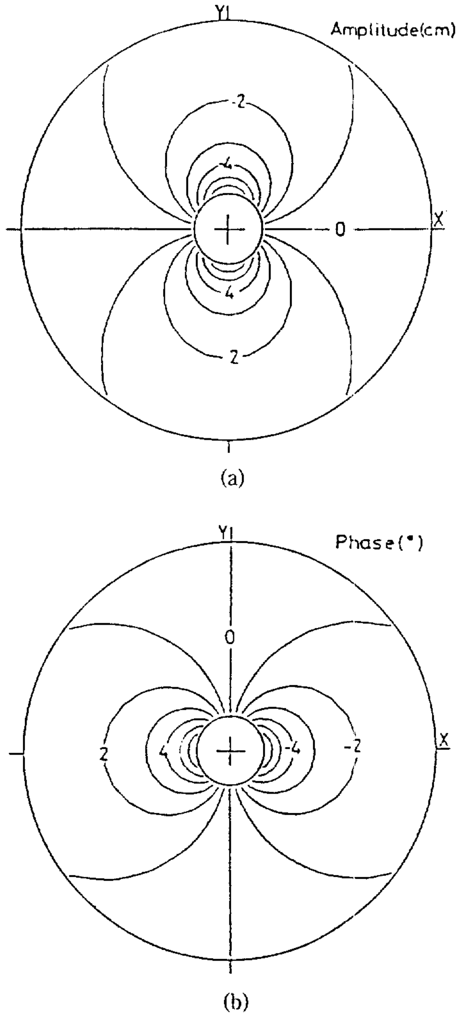

Fig. 5. Distributions of the scattered-wave amplitude (a) and phase (b) in the case of Fig. 4.

gation of the primary wave. Near the island, particulary around the northern and southern sides of the island, coamplitude lines are bent to conform to the circular coastline of island. It should be noticed that the amplitude along the coast of the island has a constant value of 100 cm. Cophase lines around the island illustrate that the wave travels much slower on the north and south coast than farther outside and much faster in the frontal and leeward coast. This results in large phase lags over the island.

Distributions of the amplitude and phase of the scattered wave are presented in Fig 5. Amplitude varies along the azimuthal direction around the island and decreases with distance from the island. The largest amplitude at the coast is about 7 cm, and the signs of amplitude are opposite in both sides of the island. The scattered wave phase propagates from the front coast of the island towards the leeward coast and radiates offshore. The phase of the scattered wave contributes to the more rapid travel of the total wave in both coasts of the island in Fig. 4(b).

The wave field of a Kelvin wave subject to bottom friction is presented in Fig. 6. Notice that the

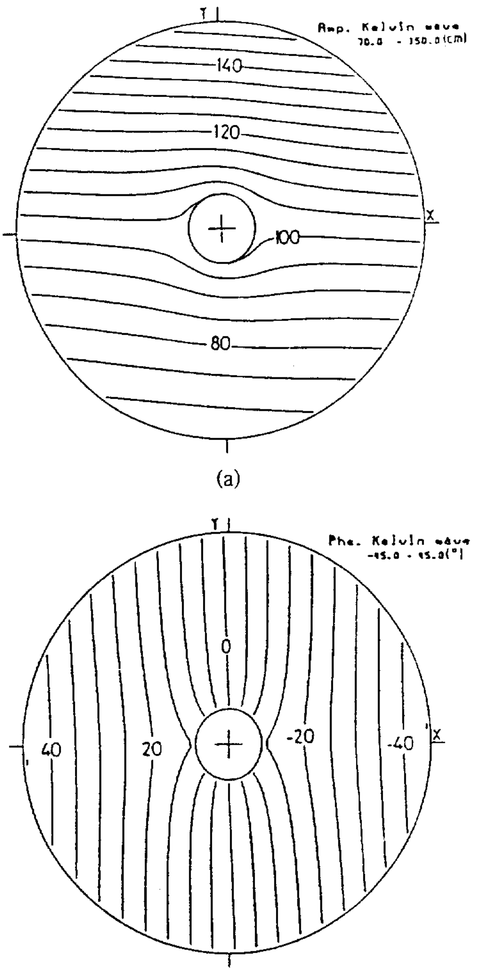

Fig. 6. Distributions of total amplitude (a) and phase (b) by the scattering of the M_2 tidal frequency Kelvin wave subject to bottom friction (C_b=0.106 cm/sec).

coamplitude lines are tilted clockwise, compared to Fig. 4. This change of amplitude distribution indicates that the amplitude is basically attenuated from east to west along the wave propagation. The contour line of 100 cm amplitude ends at the northernmost ($\theta=\pi/2$) and southernmost ($\theta=-\pi/2$) point of the island so that the amplitude attenuation becomes symmetric along northern and southern coast of the island. Amplitude variation along the coast of the island will be determined by the radius of island and by the damping coefficient, which appears in (13). The phase lines off-

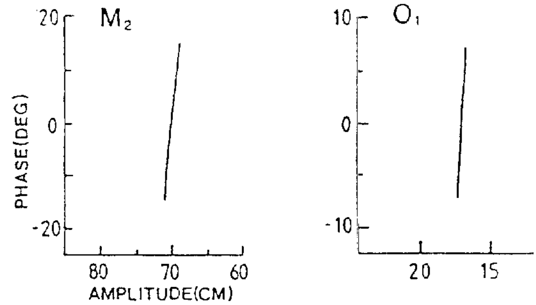

Fig. 7. Amplitude-phase diagrams using the values at the circumference of the island in the case of the scattering of the M_2 and O_1 tidal frequency Kelvin wave subject to bottom friction.

shore are a little changed, compared to those in Fig. 4. This change is made with the wavenumber m in (14). However, the change of phase distribution around the island can not be perceived. The bottom friction increases the wavenumber , but the increase of phase lag over the small distance of the island diameter is very small compared to that in an inviscid fluid.

Amplitude-phase diagram

To examine the variations of amplitude and phase along the coast of the island due to bottom friction, amplitude-phase diagrams are constructed for M_2 and O_1 tide-frequency waves subject to bottom friction with C_b=0.106 cm/sec (Fig. 7). The wave amplitudes of the M_2 and O_1 tide are calculated by multiplying (13) by 70.0 cm and 17.2 cm respectively. In our example case, the O_1 tide is subinertial frequency wave and the M_2 tide is superinertial.

The amplitude-phase relationships for M_2 and O_1 are linear, indicating that the amplitudes are symmetric along both side coasts of island from the frontal to leeward shore (i.e., symmetric relative to the propagation direction). For both tides, the amplitudes in the negative phase are lager than those in the positive phase even though the amplitude difference is very small (about 4% of incident (mean) amplitude). The slight clockwise tilt of the amplitude-phase line relative to the phase axis implies an amplitude attenuation from the frontal to leeward coast (Of course, the lines will be parallel to the phase axis when bottom friction is neglected). The maximum phase difference for the M_2 tide is about 35 degrees, which is twice that of the O1 tide. This is consistent with characteristics of long-wave propagation. However, the fact that both tides exhibit similar amplitude-phase relationship in Fig. 7 implies that the scattering character of both tidal-frequency Kelvin waves is basically the same.

CONCLUSION AND DISCUSSION

This paper presents an approximate solution for the case of Kelvin wave incident on a small cylindrical island. In the case of an inviscid fluid, the resultant scattering produces a uniform amplitude along the coast of the island. In the presence of bottom friction, the symmetry of wave amplitude along both coasts is retained while the amplitude attenuates along both coasts in the direction of wave propagation. The scattering also makes the wave travel more rapidly in the front and leeward coasts than farther offshore.

This amplitude variation of the Kelvin wave along the coast of the island is very different from that of Sverdrup wave, which makes the amplitude-phase relationship elliptic (unsymmetric) in shape due to geographical variation of amplitude along the coast (Kim and Lee, 1986; Defant, 1960). Moreover, the amplitude variation of Kelvin wave can not be produced without bottom friction while that of Sverdrup wave can be produced in the case of an inviscid fluid. The dynamical process that the Coriolis force produce the symmetric amplitude variation of Kelvin wave along the island coast is very similar with the case of Sverdrup wave even though the pattern of amplitude variation for both waves is quite different.

Proudman (1914) derived a solution for the diffraction of a Kelvin wave by a semi-elliptic cape on a straight coast. The solution shows that the wave amplitude does not vary along the coast of the cape in an inviscid fluid. Our theoretical results for scattering without friction is consistent with Proudman's solution.

The scattering solution (13) and (14) is linear for the spatial functions so that the distributions of amplitude and phase will be determined by the wavenumbers of the incident Kelvin wave. Mofjeld (1980, Fig. 8) showed that β is always smaller than n though β and n increase with increasing bottom friction and decrease with decreasing wave frequency. This implies that the bottom friction always slants the coamplitude lines of the incident Kelvin wave backward relative to the direction of wave propagation. Mofjeld (1980) pointed out that a larger friction will slant the cophase lines of the Kelvinwave more backward relative to the wave propagating direction since m increases with friction. In the case of large friction, the distribution of coamplitude and cophase lines in Fig. 6 will be changed. However, the amplitude-phase relationship remains a straight line, because the amplitude variation with attenuation along the coast of the island is a function of $\cos\theta$ in (13), which is even in θ. Increase in bottom friction will cause a larger clockwise tilt in the amplitude-phase relation shown in Fig. 7.

The scattering solution for a Kelvin wave considered in this paper may be applied around Cheju Island, because it indicates a possibility that a free wave in the subinertial frequency range can propagate around an island. Since the amplitude of diurnal tides decreases southward away from the southern coast of Korea in general (Lee and Kim, 1988), Kelvin wave is probably a good propagator of subinertial tides in this region. However, it is noticed that the solution does not fully explain the observed relationship between amplitude and phase around Cheju Island. The amplitude-phase diagram by Lee and Kim (1988) is ellipic, whereas the theoretical one shown in Fig. 7 is linear.

The major difference between the tides observed around Cheju Island and Kelvin wave seems the type of currents. Currents simulated numerically by Choi(1988) are of a rotary type, which indicates that some parts of tidal currents around Cheju Island have characteristics of Sverdrup or Poincare wave. However, currents associated with Kelvin wave are rectilinear. Apparently currents around Cheju Island are not of a pure Kelvin wave. Lee and Kim (1988) ascribed the differential variation of diurnal tide amplitude around Cheju Island to the conversion of rotary currents into rectilinear currents near the coast of the island. Further progress to understand dynamics of tidal currents around Cheju Island may be made by developing a scattering theory for subinertial long waves of rotary currents.

ACKNOWLEDGEMENTS

We are deeply thankful to Dr. Robert C. Beardsley at WHOI and Mrs. Lorraine Towle for critical and careful reading of the manuscript. Helps by Yang-Ki Cho to prepare the final manuscript are greatly appreciated. This research has been supported by the Korean Science and Engineering Foundation and by Dae Woo Foundation.

REFERENCES

Choi, B. H., 1980. A Tidal Model of the Yellow Sea and the East China Sea. Korea Ocean Res. Dev. Inst. Rept., KORDI-80-02, 72pp.

Defant, A., 1961. Physical Oceanography. Vol.II. Pergamon Press, 598pp.

Kim, K. and S. H. Lee, 1986. Variation of the M_2 Tide Amplitude around Jeju-Do. J. Oceanol. Soc. Korea, **21**: 171-183.

Larsen, J. C., 1977. Cotidal Charts for the Pacific Ocean near Hawaii using f-plane Solutions. J. Phys. Oceanogr., **7**: 100-109.

Le Blond, P. H. and L. A. Mysak, 1978. Waves in the Ocean. Elsevier Oceanogr. Ser., No. 20, 602pp.

Lee, S. H. and K. Kim, 1988. Variations of the Diurnal Tides around Jeju-Do. J. Oceanol. Soc. Korea, **23**: 62-69.

Longuet-Higgins, M. S., 1970. Steady Currents Induced by Oscilations round Islands. J. Fluid Mech., **42**: 701-720.

Mofjeld, H. O., 1980. Effects of Vertical Viscosity on Kelvin Waves. J. Phys. Oceanogr., **10**: 1039-1050.

Pedlosky, J., 1979. Geophysical Fluid Dynamics. Springer-Verlag, New York, pp. 624.

Platzman, G. W., 1971. Ocean Tides and Related Waves. In: W. H. Reid (ed), Mathematical Problems in the Geophysical Sciences. Amer. Math. Soc., Providence, **2**: 239-291.

Proudman, J., 1914. Diffraction of Tidal Waves on Flat Rotating Sheet of Water. Proc. Lond. Math.Soc., 2nd ser., **14**: 89-102.

Accepted July 31, 1993